Published in final edited form as:
Science. 2014 August 1; 345(6196): 535–542. doi:10.1126/science.1253994.

Decreased motivation during chronic pain requires long-term depression in the nucleus accumbens

Neil Schwartz[1], **Paul Temkin**[1], **Sandra Jurado**[1,2], **Byung Kook Lim**[1,3], **Boris D. Heifets**[1], **Jai S. Polepalli**[1], and **Robert C. Malenka**[1,*]

[1]Nancy Pritzker Laboratory, Department of Psychiatry and Behavioral Sciences, Stanford University School of Medicine, 265 Campus Drive, Stanford, CA 94305, USA

[2]Department of Pharmacology, School of Medicine, University of Maryland, 655 West Baltimore Street, Baltimore, MD 21201, USA

[3]Neurobiology Section, Division of Biological Sciences, University of California, San Diego, La Jolla, CA 92093, USA

Abstract

Several symptoms associated with chronic pain, including fatigue and depression, are characterized by reduced motivation to initiate or complete goal-directed tasks. However, it is unknown whether maladaptive modifications in neural circuits that regulate motivation occur during chronic pain. Here, we demonstrate that the decreased motivation elicited in mice by two different models of chronic pain requires a galanin receptor 1–triggered depression of excitatory synaptic transmission in indirect pathway nucleus accumbens medium spiny neurons. These results demonstrate a previously unknown pathological adaption in a key node of motivational neural circuitry that is required for one of the major sequela of chronic pain states and syndromes.

Symptoms that profoundly affect the quality of life of patients with chronic pain include fatigue, reductions in pre-pain activities, and depression (1–4). A common feature of these symptoms is a decrease in the motivation to undertake and to successfully complete goal-directed actions. Although in the setting of acute pain these features may be adaptive by limiting activity during the healing process and reducing the likelihood of future injury by motivating avoidance (5, 6), they are a major source of the morbidity accompanying chronic pain syndromes. Here, we hypothesize that like the maladaptive neural plasticity that contributes to somatosensory symptoms of chronic pain (7, 8), concurrent maladaptive plasticity occurs in neural circuits that regulate motivation. Therefore, we focused on the nucleus accumbens core (NAc) because it is a key node of the neural circuits mediating

*Corresponding author: malenka@stanford.edu.

SUPPLEMENTARY MATERIALS
www.sciencemag.org/content/345/6196/535/suppl/DC1
Materials and Methods
Figs. S1 to S10
References (*49–54*)

motivated behaviors (9–11), and activity within the human NAc correlates with both the subjective experience of pain as well as the transition to chronic pain (12, 13).

Chronic pain reduces motivation in two mouse models

We used two mouse models of chronic pain (14, 15); chronic inflammatory pain induced by means of injection of complete Freund's adjuvant (CFA) into the hind paw and neuropathic pain induced by means of selective injury of the sciatic nerve (SNI). To measure motivation, we used a progressive ratio (PR) operant test in which it becomes progressively more difficult to earn each subsequent reward (16, 17). The point at which the subject gives up provides a measure of motivation to work for reward (Fig. 1, A to C). Before inducing the models, all animals made a similar number of nose pokes and earned a comparable number of rewards (over the course of the 2-day baseline period) (Fig. 1, D and E, and fig. S1A). In contrast, 7 to 21 days after induction of chronic pain, animals exhibited a ~40% drop in the number of nose pokes to earn rewards, resulting in a stable reduction in the rewards earned over the 3-week testing period (Fig. 1, F to H). There was no change in the number of searches for reward (Fig. 1I), implying that animals exhibited no change in their ability to cross the chamber to search for the reward and no change in their perceived value of the reward.

To further test the animals' valuation of rewards, on day 22 after pain induction, animals were tested on a fixed ratio 1 (FR1) schedule of reward, during which each nose poke earns a reward. Under this schedule, all groups earned the maximum number of rewards (30) at the same rate and searched for rewards a comparable number of times (fig. S1B). Similarly, neither model affected sucrose preference (Fig. 1J) or food consumption (fig. S1C).

Last, although the mechanical threshold of the animal did not predict its level of impairment on the PR task (fig. S2), we asked whether acutely suppressing the somatosensory symptoms of the models would ameliorate the observed reduction in motivation. In two subsets of animals after CFA and after SNI induction, the analgesics diclofenac and clonidine, respectively, were administered before testing on day 15. Despite an increase in paw withdrawal thresholds in both pain models (Fig. 1K), neither acute analgesic ameliorated performance on the PR task (Fig. 1L).

Chronic pain elicits synaptic modifications in nucleus accumbens

To determine whether chronic pain elicits synaptic changes in NAc circuitry, we prepared brain slices from bacterial artificial chromosome (BAC) transgenic animals and made targeted whole-cell recordings from visually identified medium spiny neurons (MSNs) belonging to either the direct pathway, D1 dopamine receptor expressing MSNs (D1-MSNs), or the indirect pathway, D2 dopamine receptor expressing MSNs (D2-MSNs) (18). We first calculated the ratio of α-amino-3-hydroxy-5-methyl-4-isoxazolepropionic acid receptor (AMPAR)–mediated excitatory postsynaptic currents (EPSCs) to *N*-methyl-D-aspartate receptor (NMDAR)–mediated EPSCs (AMPAR/NMDAR ratio). Seven to 12 days after either CFA injection or SNI surgery, this ratio was significantly lower in NAc D2-MSNs but was unchanged in NAc D1-MSNs (Fig. 2, A to C). This decrease in the two models was at least in part due to a decrease in the number and/or function of AMPARs

because the amplitude of miniature EPSCs (mEPSCs) was decreased in D2-MSNs but not in D1-MSNs (Fig. 2, D, F, and G). In contrast, assays of presynaptic function were not affected in either model (Fig. 2E and fig. S3).

The fractional decrease for D2-MSN mEPSC amplitudes in both models was less than the fractional decrease in the AMPAR/NMDAR ratios, suggesting that chronic pain may have also affected NMDAR-mediated synaptic transmission. We therefore recorded pharmacologically isolated NMDAR EPSCs and found that their time constant of decay was prolonged in D2-MSNs, but not D1-MSNs, in NAc slices prepared 7 to 12 days after model induction (Fig. 2, H and I). Prolonged NMDAR EPSC decay kinetics are normally due to an increase in the proportion of synaptic NMDARs containing the GluN2B subunit (19). We confirmed this possibility; the GluN2B antagonist ifenprodil caused a larger depression of NMDAR EPSCs in D2-MSNs 7 to 12 days after induction as compared with that of controls (Fig. 2, J and K). This difference was not observed in D1-MSNs (Fig. 2K).

In the early stages of withdrawal from drugs of abuse, a change in the stoichiometry of synaptic NMDARs in MSNs can be observed, and this is followed at later time points by modulation of AMPAR-mediated transmission (20). To determine whether similar changes occur at the onset of the pain experience, we repeated the assays of synaptic function at 12 hours after injection of CFA (CFA12hrs). At this early time point, AMPAR-mediated synaptic transmission was unchanged compared with controls (Fig. 3, A to E), yet NMDAR EPSCs exhibited prolonged decay kinetics in D2-MSNs (Fig. 3, F and G).

Galanin is required for pain-induced synaptic modifications in NAc

In several brain regions, activation of G protein–coupled receptors (GPCRs) by different neuromodulators causes changes in synaptic NMDAR stoichiometry (19). We investigated the possible role of the neuropeptide galanin (Gal) in the pain-induced changes in NMDAR stoichiometry in NAc D2-MSNs for several reasons. In patients, polymorphisms affecting Gal signaling predict the development of comorbidities during chronic pain, increased reactivity in the NAc to rewards, and poor resilience to long-term stress (21–24). In rodents, intraventricular infusion of Gal reduces performance on a PR task (25), and in several pain models, Gal is up-regulated in brain regions that project to NAc (26–29). We observed Gal-positive neurons, which were retrogradely labeled by a rabies virus injected into the NAc (30), in several brain regions (Fig. 4A). Also consistent with previous studies (31, 32), in both D1-MSNs and D2-MSNs Gal (1 μM) caused a transient, presynaptic decrease in excitatory transmission, which was unaffected by loading MSNs with guanosine 5′-*O*-(2′-thiodiphosphate) (GDP-β-S) to inhibit GPCR signaling in post-synaptic compartments (Fig. 4B and figs. S4 and S5) (31). In contrast to this transient change, the decay kinetics of NMDAR EPSCs in D2-MSNs but not D1-MSNs were prolonged after Gal application (Fig. 4C and fig. S5). This change in NMDAR EPSC decay kinetics was blocked by postsynaptic GDP-β-S (fig. S5) and was accompanied by an increase in the magnitude of the NMDAR EPSC depression caused by ifenprodil in D2-MSNs only (Fig. 4D).

To directly test whether Gal signaling within the NAc is required for the change in NMDAR EPSC kinetics in D2-MSNs, we used two complementary approaches. In one set of animals,

we infused the galanin receptor 1,2 (GalR1,2) antagonist M40 (0.4 μg μL^{-1}) into the NAc preceding and during the 12-hour period after CFA treatment. In another set of animals, before CFA treatment we expressed an effective short hairpin RNA (shRNA) to GalR1 in the NAc bilaterally because GalR1, but not GalR2, has been implicated in regulating motivation (Fig. 4E) (25). We chose CFA injections because the symptoms develop and plateau rapidly, producing a temporally more well-defined model of chronic pain (14, 33). Both manipulations prevented the increase in NMDAR EPSC decay kinetics in D2-MSNs normally caused by CFA treatments, whereas intra-NAc injection of vehicle alone did not (Fig. 4, F to H). Furthermore, knockdown of GalR1 prevented the increased sensitivity to ifenprodil caused by CFA injection (Fig. 4I).

The results thus far suggest that during the onset of chronic pain, Gal in the NAc signals through GalR1 to increase the synaptic fraction of GluN2B in D2-MSNs. Then over the ensuing 1 to 2 weeks, AMPAR-mediated synaptic transmission progressively decreases. In other brain regions, a similar change in NMDAR stoichiometry has been suggested to reduce the threshold for induction of long-term depression (LTD) of AMPAR-mediated transmission (34). Consistent with this hypothesis, preincubating NAc slices in Gal increased the magnitude of LTD elicited in D2-MSNs (fig. S6, A to C). NMDAR-dependent LTD in control slices was blocked by D-AP5 (fig. S6, D and E) but was unaffected by ifenprodil, whereas in Gal-treated slices, ifenprodil strongly inhibited LTD (fig. S7). Three findings suggest that similar events occur in vivo in the NAc in the pain models. First, in both models knockdown of GalR1 in vivo prevented the decrease in AMPAR/ NMDAR ratios in NAc D2-MSNs (Fig. 5, A and B). Second, NMDAR-dependent LTD in D2-MSNs was reduced—presumably occluded—in slices prepared from animals 7 to 12 days after model induction (Fig. 5, C to E). Third, the reduction in LTD that occurs in the chronic-pain models was reversed in D2-MSNs in which knockdown of GalR1 occurred (Fig. 5, D and E).

NAc synaptic modifications required for decreased motivation during chronic pain

To determine whether GalR1-dependent synaptic changes in NAc are necessary for the decreased motivation accompanying the chronic pain models, we performed behavioral assays in animals that had been injected bilaterally into the NAc with viruses expressing enhanced green fluorescent protein (eGFP) alone, the GalR1 shRNA, or the GalR1 shRNA along with a GalR1-eGFP replacement construct (Rep.GalR1 KD) (Fig. 5, F and G). Behavior during baseline PR testing was similar between groups (Fig. 5H), and after model induction, a new set of control animals (uninjected or expressing eGFP alone) showed comparable decreases in motivation to nose poke for rewards (Fig. 5, I and J). Therefore, these groups were combined. Knockdown of GalR1 bilaterally in the NAc ameliorated the decrease in motivation normally caused by both pain models (Fig. 5, I and J), whereas expression of the Rep. GalR1 knockdown in CFA-treated animals returned their behavior to that resembling control animals: They exhibited a decrease in nose pokes after model induction (Fig. 5I). To limit the expression of the replacement GalR1 construct to indirect pathway NAc MSNs, we injected a CRE-dependent Rep.GalR1 KD construct into the NAc

of Adenosine A2a CRE mice, in which CRE expression is limited to D2-MSNs (35). These animals exhibited a decrease in nose pokes after SNI comparable with the decrease observed in controls after SNI (fig S8). Somatosensory symptoms and other measures of operant behavior were not affected by the knockdown of GalR1 in either model (fig. S9).

To determine whether the depression of AMPAR-mediated transmission and reduction/ occlusion of LTD were required for the pain-induced behavioral changes, we took advantage of the finding that NMDAR-dependent LTD depends on the appropriate synaptic positioning of the critical phosphatase calcineurin (PP2B) by the scaffolding protein A-kinase anchoring protein 79/150 (AKAP) (36). Thus, we knocked down AKAP in the NAc and replaced it with a mutant AKAP that does not bind PP2B (AKAPΔPP2B), a manipulation that blocks LTD in the hippocampus (36). This manipulation inhibited LTD in NAc MSNs, whereas replacement of AKAP with a shRNA-resistant wild-type AKAP (AKAPWT) did not (Fig. 6, A to C). Although the basal AMPAR/ NMDAR ratio in D2-MSNs was not affected by AKAPΔPP2B, the decrease in this ratio elicited by the CFA model was inhibited (Fig. 6D).

Next, we repeated the behavioral experiments in animals expressing the AKAP replacement constructs in the NAc bilaterally (Fig. 6E). These manipulations did not affect the behavioral responses during baseline PR testing (Fig. 6F and fig. S10). However, whereas animals expressing control constructs (AKAPWT and eGFP) exhibited the expected decrease in nose pokes after model induction, animals expressing AKAPΔPP2B showed no deficits in performance (Fig. 6, G and H). Thus, in two different pain models, two different molecular manipulations (GalR1 knockdown and AKAPΔPP2B), which prevented chronic pain–induced modifications of excitatory synapses on NAc D2-MSNs via completely independent mechanisms, prevented pain-induced motivational impairments (Fig. 6I) while having no effect on mechanical thresholds or other measures of operant goal-directed behaviors (figs. S9 and S10).

Discussion

The NAc is a key node of the neural circuitry that regulates motivation (10). Manipulations that disrupt its activity appear to impair performance on more difficult operant tasks but have little effect on the performance of easy operant tasks, perhaps because impairments of NAc function bias behavioral choices to those that require less effort (9, 37–39). Here, we demonstrate that two different chronic pain models cause a selective impairment in performance on a difficult PR task but have no detectable effects on easier tasks or the value of rewards. This chronic pain–induced decrease in motivation requires a decreased excitatory drive onto indirect pathway NAc MSNs downstream of activation of the neuropeptide receptor GalR1 via a cascade of synaptic modifications (Fig. 6J).

Simple models proposing a dichotomous role for striatal indirect and direct pathways have been useful in generating hypotheses with which to describe the circuit adaptations underlying behaviors associated with models of addiction and depression (30, 40). However, they are inadequate to account for the diverse actions of neuropeptides on NAc synaptic and circuit function (30, 41–44) as well as the neuronal activity observed during operant behaviors (45, 46). Nonetheless, the present findings—along with the observations that

reductions in effortful behavior are caused by blocking D2 receptors in NAc and that these effects can be reversed by A2a receptor antagonists (38, 39)—support a key role of NAc D2-MSNs in regulating performance during more difficult tasks. Because the NAc integrates inputs from multiple structures, future studies will need to address the critical question of whether the chronic pain–induced synaptic changes are global, affecting all excitatory inputs onto MSNs, or rather are input-specific.

Previous studies on mouse models of chronic pain report no change in home cage behaviors or measures of affective behaviors during the first month of the pathology (14, 15). Within a similar time frame, by focusing on a more subtle aspect of goal-directed operant behavior—the motivation to work for natural reward—we found that motivation was impaired. Our results suggest that pain-induced synaptic adaptations within the NAc contribute to a subjective impairment in the ability to initiate or sustain physical or mental tasks (47, 48), or to the symptom of central fatigue commonly reported by chronic pain patients (1, 2). These results also suggest specific synaptic targets that may be susceptible to therapeutic interventions.

Supplementary Material

Refer to Web version on PubMed Central for supplementary material.

Acknowledgments

We thank members of the Malenka lab for helpful feedback and comments during the study. We thank S. Fang and A. Darvishzadeh for help with stereotaxic injections and P. Rothwell for setting up the operant behavior chambers and software. This work was supported by a Banting postdoctoral fellowship (N.S.) and the NIH (R.C.M.). All primary data (behavioral, electrophysiological, and immunohistochemical) are archived in the Department of Psychiatry and Behavioral Sciences, Stanford University School of Medicine.

REFERENCE AND NOTES

1. Nicholson B, Verma S. Pain Med. 2004; 5:S9–S27. [PubMed: 14996227]
2. Turk DC, Audette J, Levy RM, Mackey SC, Stanos S. Mayo Clin Proc. 2010; 85:S42–S50. [PubMed: 20194148]
3. Dersh J, Polatin PB, Gatchel RJ. Psychosom Med. 2002; 64:773–786. [PubMed: 12271108]
4. Jonsson T, et al. Acta Anaesthesiol Scand. 2011; 55:69–74. [PubMed: 21039361]
5. Johansen JP, Fields HL, Manning BH. Proc Natl Acad Sci USA. 2001; 98:8077–8082. [PubMed: 11416168]
6. Borsook D, et al. Eur J Pain. 2007; 11:7–20. [PubMed: 16495096]
7. von Hehn CA, Baron R, Woolf CJ. Neuron. 2012; 73:638–652. [PubMed: 22365541]
8. Basbaum AI, Bautista DM, Scherrer G, Julius D. Cell. 2009; 139:267–284. [PubMed: 19837031]
9. Salamone JD, Correa M. Neuron. 2012; 76:470–485. [PubMed: 23141060]
10. Mogenson GJ, Jones DL, Yim CY. Prog Neurobiol. 1980; 14:69–97. [PubMed: 6999537]
11. Balleine BW, O'Doherty JP. Neuropsychopharmacology. 2010; 35:48–69. [PubMed: 19776734]
12. Scott DJ, Heitzeg MM, Koeppe RA, Stohler CS, Zubieta JK. J Neurosci. 2006; 26:10789–10795. [PubMed: 17050717]
13. Baliki MN, et al. Nat Neurosci. 2012; 15:1117–1119. [PubMed: 22751038]
14. Urban R, Scherrer G, Goulding EH, Tecott LH, Basbaum AI. Pain. 2011; 152:990–1000. [PubMed: 21256675]
15. Yalcin I, et al. Biol Psychiatry. 2011; 70:946–953. [PubMed: 21890110]

16. Roane HS. J Appl Behav Anal. 2008; 41:155–161. [PubMed: 18595280]
17. O'Brien CP, Gardner EL. Pharmacol Ther. 2005; 108:18–58. [PubMed: 16183393]
18. Shuen JA, Chen M, Gloss B, Calakos N. J Neurosci. 2008; 28:2681–2685. [PubMed: 18337395]
19. Sanz-Clemente A, Nicoll RA, Roche KW. Neuroscientist. 2013; 19:62–75. [PubMed: 22343826]
20. Lee BR, Dong Y. Neuropharmacology. 2011; 61:1060–1069. [PubMed: 21232547]
21. Max MB, et al. Mol Pain. 2006; 2:14. [PubMed: 16623937]
22. Unschuld PG, et al. J Affect Disord. 2008; 105:177–184. [PubMed: 17573119]
23. Wray NR, et al. Mol Psychiatry. 2012; 17:36–48. [PubMed: 21042317]
24. Nikolova YS, Singhi EK, Drabant EM, Hariri AR. Genes Brain Behav. 2013; 12:516–524. [PubMed: 23489876]
25. Anderson ME, Runesson J, Saar I, Langel U, Robinson JK. Behav Brain Res. 2013; 239:90–93. [PubMed: 23142608]
26. Sergeyev V, Broberger C, Hökfelt T. Brain Res Mol Brain Res. 2001; 90:93–100. [PubMed: 11406287]
27. Imbe H, et al. Neurosci Lett. 2004; 368:102–106. [PubMed: 15342143]
28. Nishii H, Nomura M, Aono H, Fujimoto N, Matsumoto T. Regul Pept. 2007; 141:105–112. [PubMed: 17335920]
29. Gu XL, Sun YG, Yu LC. Behav Brain Res. 2007; 179:331–335. [PubMed: 17383023]
30. Lim BK, Huang KW, Grueter BA, Rothwell PE, Malenka RC. Nature. 2012; 487:183–189. [PubMed: 22785313]
31. Dong Y, Tyszkiewicz JP, Fong TM. J Neurophysiol. 2006; 95:3228–3234. [PubMed: 16481456]
32. Einstein EB, Asaka Y, Yeckel MF, Higley MJ, Picciotto MR. Eur J Neurosci. 2013; 37:1541–1549. [PubMed: 23387435]
33. Cobos EJ, et al. Pain. 2012; 153:876–884. [PubMed: 22341563]
34. Yashiro K, Philpot BD. Neuropharmacology. 2008; 55:1081–1094. [PubMed: 18755202]
35. Durieux PF, et al. Nat Neurosci. 2009; 12:393–395. [PubMed: 19270687]
36. Jurado S, Biou V, Malenka RC. Nat Neurosci. 2010; 13:1053–1055. [PubMed: 20694001]
37. Nicola SM. J Neurosci. 2010; 30:16585–16600. [PubMed: 21147998]
38. Farrar AM, et al. Neuroscience. 2010; 166:1056–1067. [PubMed: 20096336]
39. Santerre JL, et al. Pharmacol Biochem Behav. 2012; 102:477–487. [PubMed: 22705392]
40. Lobo MK, Nestler EJ. Front Neuroanat. 2011; 5:41. [PubMed: 21811439]
41. Lemos JC, et al. Nature. 2012; 490:402–406. [PubMed: 22992525]
42. Land BB, et al. J Neurosci. 2008; 28:407–414. [PubMed: 18184783]
43. Dölen G, Darvishzadeh A, Huang KW, Malenka RC. Nature. 2013; 501:179–184. [PubMed: 24025838]
44. Marinelli M, Piazza PV. Eur J Neurosci. 2002; 16:387–394. [PubMed: 12193179]
45. Cui G, et al. Nature. 2013; 494:238–242. [PubMed: 23354054]
46. Kasanetz F, et al. Science. 2010; 328:1709–1712. [PubMed: 20576893]
47. Chaudhuri A, Behan PO. Lancet. 2004; 363:978–988. [PubMed: 15043967]
48. Norheim KB, Jonsson G, Omdal R. Rheumatology (Oxford). 2011; 50:1009–1018. [PubMed: 21285230]

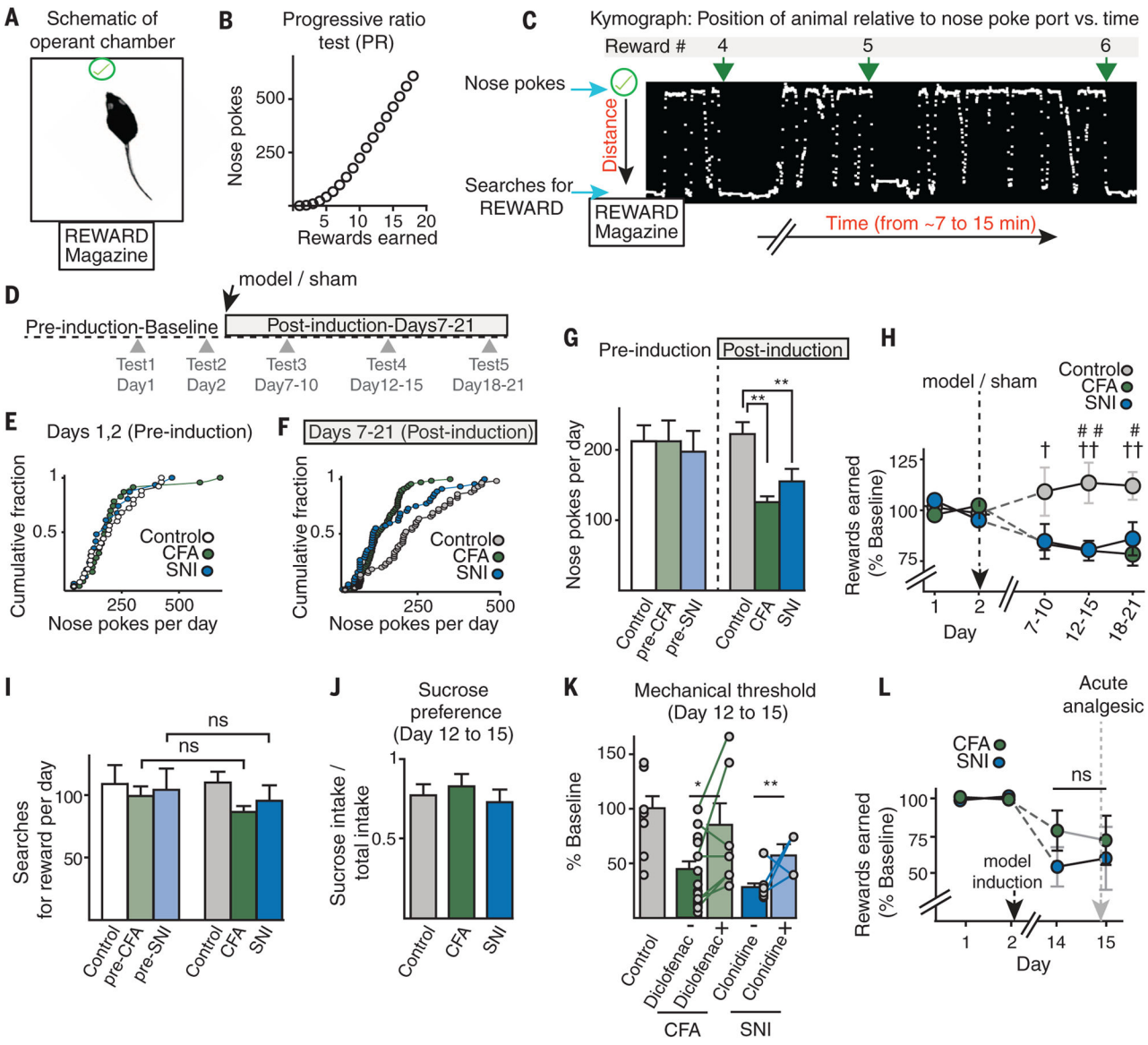

Fig. 1. Motivation is impaired in models of chronic pain

(**A**) Schematic of mouse in the operant chamber. (**B**) Sum of nose pokes required to earn rewards on PR schedule. (**C**) Kymograph illustrating distance from nose poke port (*y* axis) versus time (*x* axis). Green arrows indicate times at which rewards 4 to 6 were earned. (**D**) Time line of experiments. Results from 2 PR tests before induction of pain models were compared with results from 6 PR tests at three time points after induction. (**E**) Nose pokes per animal during 2 days of baseline testing. (**F** to **H**) Both CFA and SNI induction reduced number of nose pokes, resulting in a drop in the rewards earned at the respective time points (control, $n = 12$ mice, includes SNI sham surgery $n = 4$, CFA sham injections $n = 5$, untreated $n = 3$; CFA $n = 10$ mice; SNI $n = 8$ mice). (G) $^{**}P < 0.01$ versus control. (H) CFA $\dagger P < 0.05$, $\dagger\dagger P < 0.01$; SNI $\#P < 0.05$, $\#\#P < 0.01$; post hoc *t* tests. (**I** and **J**) During PR tests, there was no difference in searches for rewards before or after induction nor differences in the sucrose preference test (control $n = 6$ mice, CFA $n = 6$ mice, SNI $n = 5$

mice). (**K**) Both pain models reduce mechanical threshold, and this is ameliorated by analgesic administration (diclofenac, subcutaneous, $n = 8$ mice, $^{*}P < 0.05$; clonidine, intrathecal, $n = 5$ mice, $^{**}P < 0.01$; Student's t tests). (**L**) Neither acute analgesic affects the reduction in rewards earned after model induction. For all figures, error bars are SEM.

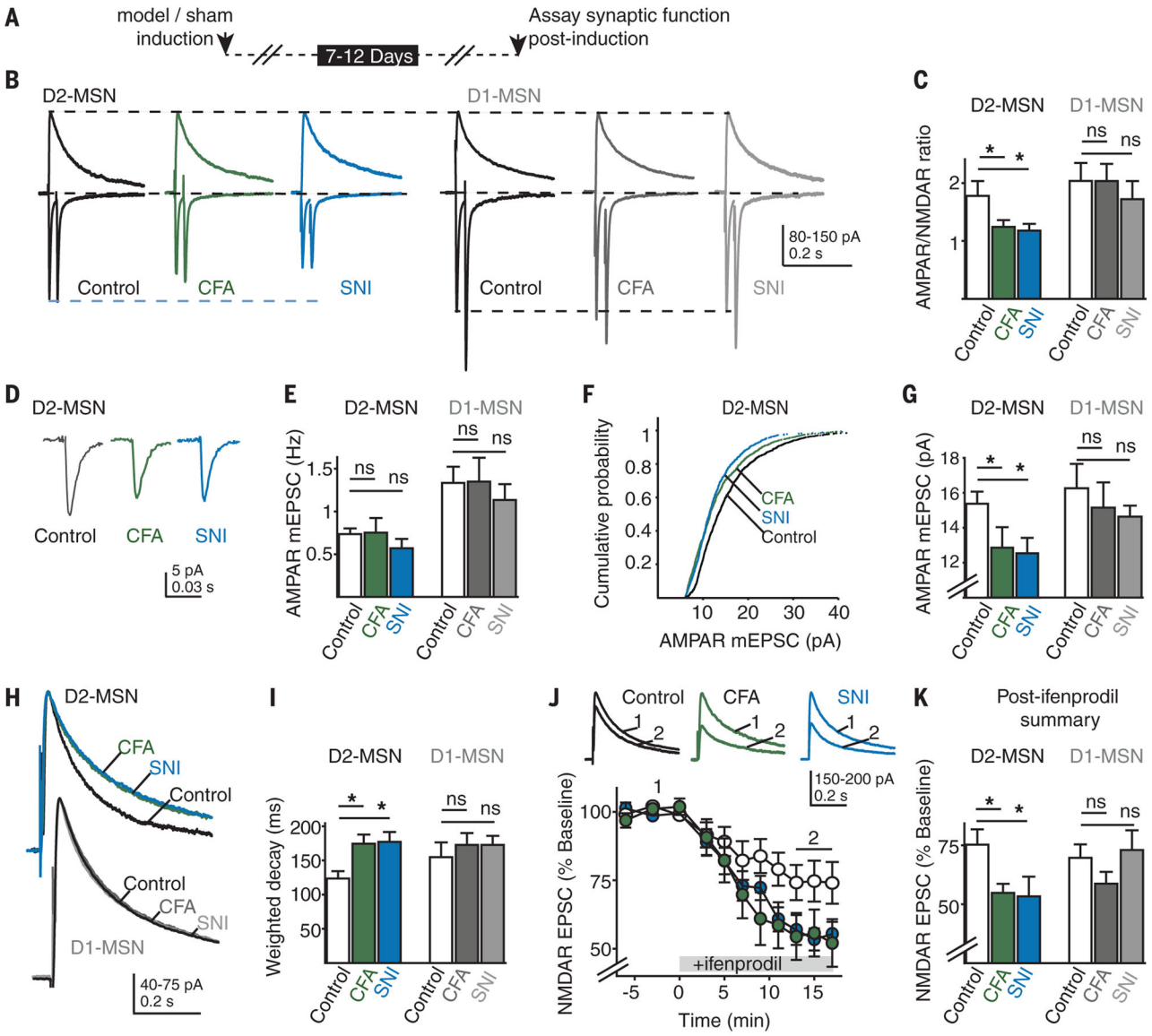

Fig. 2. Excitatory synapses are modified 7 to 12 days after induction of chronic pain

(**A**) Time course of experiments in (B) to (K). (**B**) Sample EPSCs recorded at +40 mV (top traces) and two EPSCs evoked with a 50-ms interval recorded at −70 mV (bottom traces) from NAc D2-MSNs and D1-MSNs at 7 to 12 days after sham procedures or after model induction. EPSC amplitudes are normalized to peaks at +40 mV. (**C**) Summary showing AMPAR/ NMDAR ratios in D2-MSNs and D1-MSNs in both pain models (D2, control n = 15 cells, CFA n = 13 cells, SNI n = 12 cells, *P < 0.05 post hoc t test; D1, control n = 12 cells, CFA n = 7 cells, SNI n = 11 cells). (**D**) Average traces of 100 mEPSCs from representative D2-MSNs. (**E**) mEPSC frequency was unaffected by CFA and SNI treatments. (**F** and **G**) Cumulative distribution of mEPSC amplitudes (F) and averages (G) in D2-MSNs and D1-MSNs in both pain models (D2, control n = 14 cells, CFA n = 10 cells, SNI n = 12 cells, *P < 0.05 Student's t test; D1, control n = 13 cells, CFA n = 14 cells, SNI n = 13 cells). (**H**) Sample normalized average traces of pharmacologically isolated NMDAR

EPSCs. (**I**) Summary data of NMDAR EPSC decay kinetics from D2-MSNs and D1-MSNs in both pain models (D2, control $n = 12$ cells, CFA $n = 9$ cells, SNI $n = 6$ cells,$^{*}P < 0.05$ post hoc t tests; D1, control $n = 9$ cells, CFA $n = 7$ cells, SNI $n = 12$ cells). (**J** and **K**) In both models, ifenprodil (3 μM) caused a larger depression of NMDAR EPSCs in D2-MSNs versus D1-MSNs (D2, control $n = 8$ cells, CFA $n = 8$ cells, SNI $n = 6$ cells; D1, control $n = 9$ cells, CFA $n = 7$ cells, SNI $n = 5$ cells; $^{*}P < 0.05$ post hoc t tests).

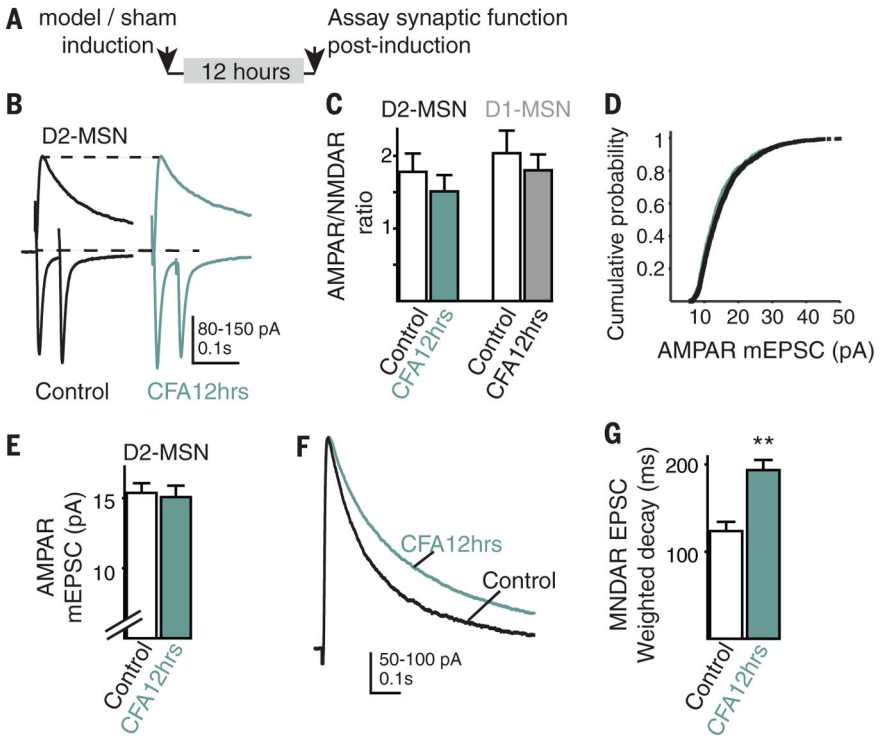

Fig. 3. NMDAR EPSCs are slower in D2-MSNs 12 hours after induction of chronic pain

(**A**) Experimental protocol. (**B**) Sample EPSCs from D2-MSNs recorded 12 hours after saline (control) or CFA injection (CFA12hrs). Traces are normalized to peak at +40 mV. (**C**) Summary of AMPAR/NMDAR ratios in D2-MSNs and D1-MSNs at this time point (D2, control, $n = 15$ cells, CFA12hrs $n = 12$ cells; D1, control $n = 12$ cells, CFA12hrs $n = 9$ cells). (**D** and **E**) Cumulative distribution and average of mEPSC amplitudes from D2-MSNs at this time point (control $n = 14$ cells, CFA12hrs $n = 10$ cells). (**F**) Sample normalized average NMDAR EPSCs from D2-MSN neurons. (**G**) Summary of NMDAR EPSC weighted decay time constants 12 hours after CFA (control $n = 12$ cells; CFA12hrs $n = 16$ cells; $^{**}P < 0.01$ Student's t test).

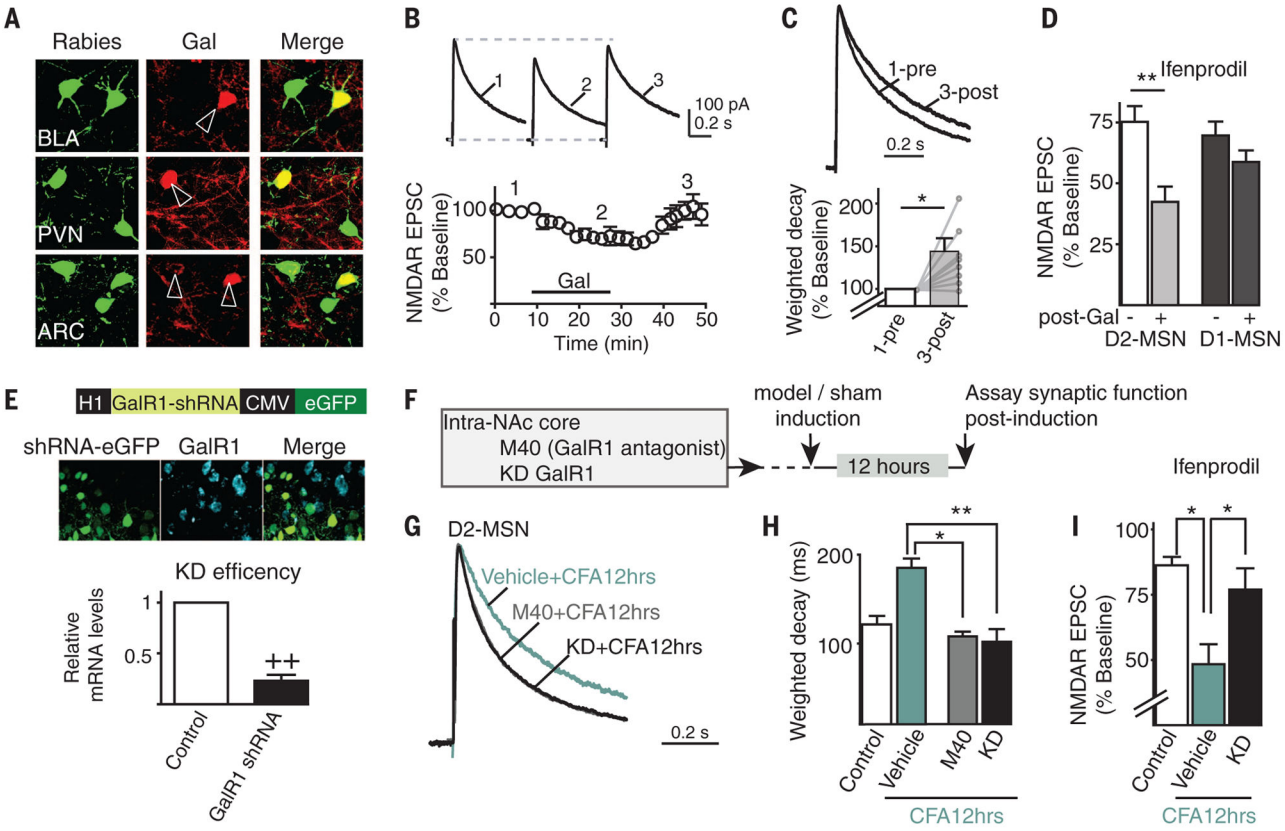

Fig. 4. Increase in NMDAR EPSC decay 12 hours after induction of chronic pain requires GalR1

(**A**) Images of neurons retrogradely labeled by rabies virus expressing eGFP (green) injected into NAc overlaid with Gal-antibody labeling (red) from basoateral amygdala (BLA), paraventricular nucleus of thalamus (PVN), and arcuate nucleus of hypothalamus (ARC). (**B**) Sample NMDAR EPSCs from D2-MSN taken at time points indicated on summary graph showing transient effects of Gal (1 μM). (**C**) Summary of change in NMDAR EPSC decay kinetics after wash-out of Gal ($n = 8$ cells; $^{*}P < 0.05$ repeated measure t test). (**D**) Ifenprodil causes larger depression of NMDAR EPSCs in D2-MSNs versus D1-MSNs from slices preincubated in Gal (D2, nontreated from Fig. 2K, post-Gal+ $n = 6$ cells; D1, nontreated from Fig. 2K, post-Gal+ $n = 6$ cells; $^{**}P < 0.01$ Student's t test). (**E**) Schematic of adeno-associated virus vector expressing GalR1 shRNA and eGPF, with images showing eGFP expression and GalR1 staining 1 month after infection of NAc. Graph shows relative mRNA levels from sister hippocampal cultures infected with eGFP and GalR1 shRNA, respectively ($n = 3$ experiments; $^{++}P = 0.006$ Student's t test). (**F**) Time line of experiments in (G) to (I). (**G**) Sample normalized NMDAR EPSCs from D2-MSNs. (**H**) Summary graph of NMDAR EPSC decay kinetics 12 hours after CFA. KD, knockdown. (D2, control taken from Fig. 3, vehicle+CFA12hrs $n = 9$ cells, M40 +CFA12hrs $n = 12$ cells, KD+CFA12hrs $n = 8$ cells; $^{**}P < 0.01$, $^{*}P < 0.05$ post hoc t tests). (**I**) Effects of ifenprodil on NMDAR EPSCs 12 hours after CFA (control n = 8 cells, Vehicle+CFA12hrs $n = 5$ cells, KD +CFA12hrs $n = 5$ cells; $^{*}P < 0.05$ post hoc t test).

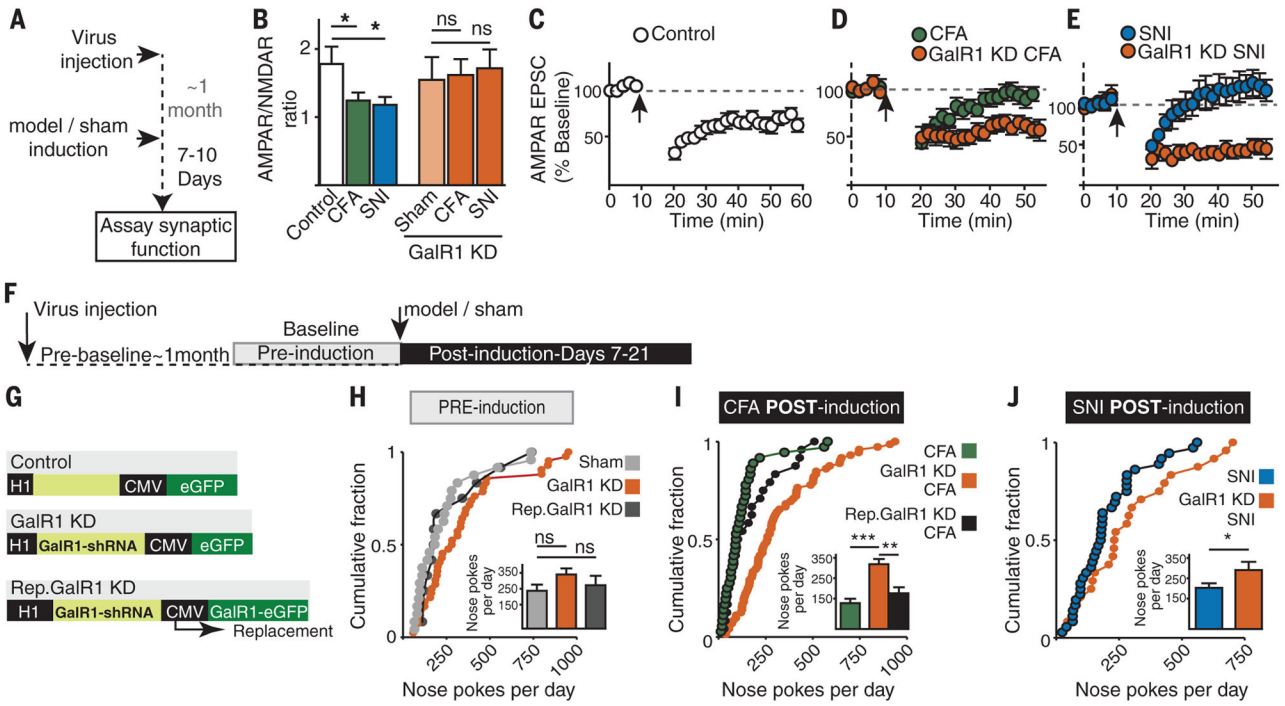

Fig. 5. GalR1 in NAc is required for pain-induced synaptic depression in D2-MSNs and reduction in motivation

(**A**) Time line of acute slice experiments in (B) to (E). (**B**) Decrease in AMPAR/NMDAR ratios in D2-MSNs in both pain models is prevented by GalR1 KD [control, CFA and SNI (left group) taken from Fig. 2; GalR1 KD, sham $n = 5$ cells, CFA $n = 11$ cells, SNI $n = 8$ cells). (**C** to **E**) Summary graphs of LTD in D2-MSNs in both pain models and effects of GalR1 KD (control, $n = 11$ cells, CFA $n = 10$ cells, GalR1 KD+CFA $n = 7$ cells, SNI $n = 6$ cells, GalR1 KD+SNI $n = 6$ cells). (**F**) Timeline of behavior experiments in (H) to (J). (**G**) Schematics of virus constructs. (**H**) Cumulative distribution of nose pokes per session and average nose pokes per day during before-induction baseline period (PRE). (sham $n = 12$ mice includes eGFP $n = 5$ mice, naive $n = 7$ mice; GalR1 KD $n = 18$ mice, Rep. GalR1 KD $n = 6$ mice). (**I** and **J**) Effects of GalR1 KD in NAc on nose pokes after model induction and rescue by coexpression of shRNA-resistant GalR1 (Rep.GalR1 KD) in CFA model. (I) CFA $n = 6$ mice includes eGFP $n = 3$ mice, naive $n = 3$ mice; GalR1 KD+CFA $n = 12$ mice, Rep. GalR1 KD+CFA $n = 6$ mice, $^{**}P < 0.01$, $^{***}P < 0.001$ Tukey's post hoc t test. (J) SNI $n = 6$ mice includes eGFP $n = 2$ mice, naïve $n = 4$ mice; GalR1 KD +SNI $n = 6$ mice, $^{*}P < 0.05$ Student's t test.

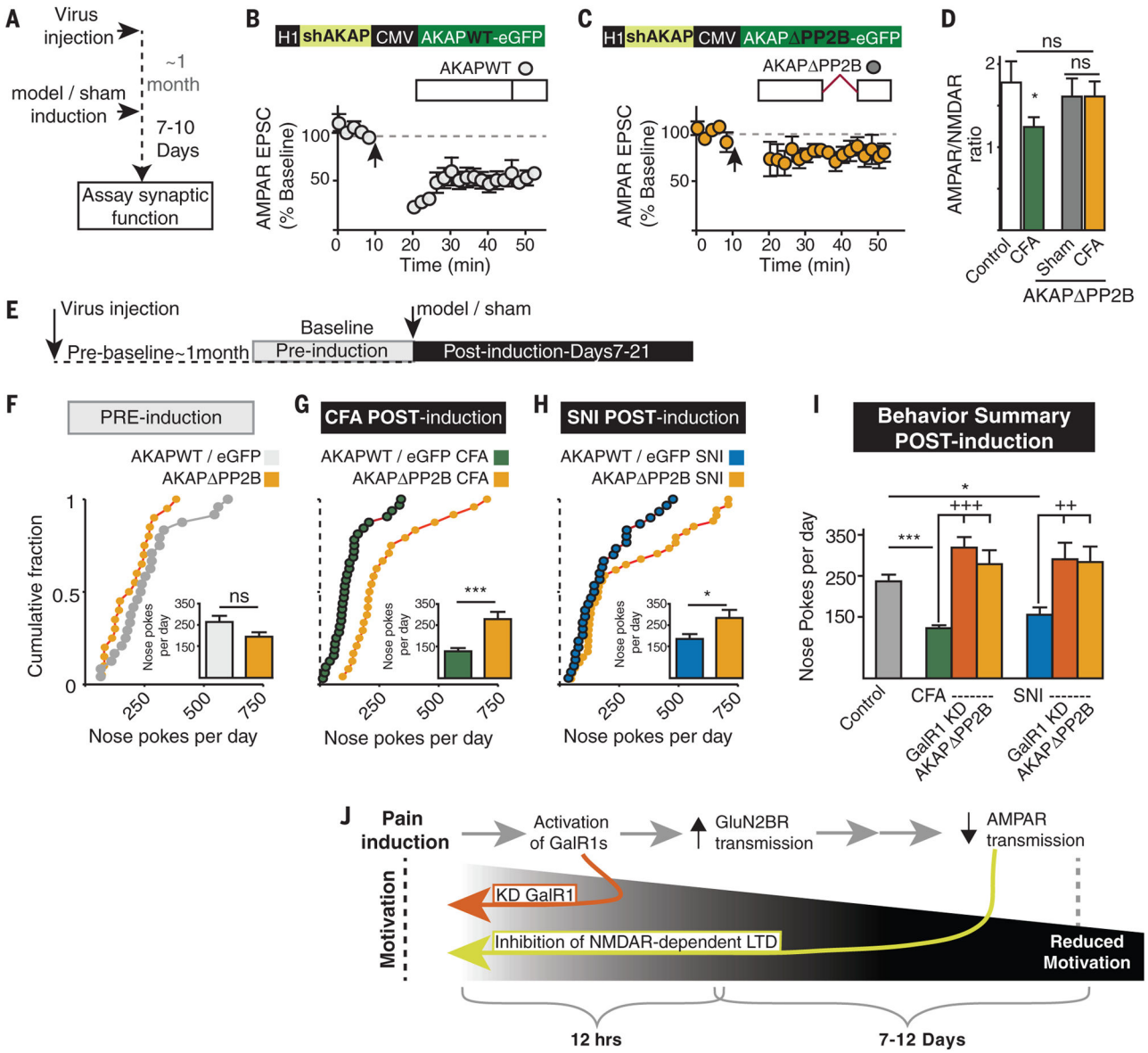

Fig. 6. NMDAR-dependent LTD in NAc is required for pain-induced decrease in motivation

(**A**) Timeline for virus injection and acute slice experiments in (B) to (D). (**B** and **C**) Schematics of AKAP replacement constructs and summary LTD graphs for D2-MSNs expressing these constructs (AKAPWT $n = 4$ cells; AKAPΔPP2B $n = 8$ cells). (**D**) Summary of AMPAR/NMDAR ratios in D2-MSNs after CFA treatment (control and CFA from Fig. 2; AKAPΔPP2B, sham $n = 7$ cells, CFA $n = 9$ cells). (**E**) Timeline for behavior experiments in (F) to (I). (**F** to **H**) Cumulative distribution of nose pokes per session and average nose pokes per day during before-induction baseline (PRE) and after model induction (POST). (F) AKAPWT/eGFP $n = 13$ mice includes eGFP $n = 5$ mice, AKAPWT $n = 8$ mice; AKAPΔPP2B $n = 10$ mice. (G) AKAPWT/eGFP CFA $n = 7$ mice includes eGFP $n = 3$ mice, AKAPWT, $n = 4$ mice; AKAPΔPP2B+CFA $n = 4$. (H) AKAPWT/eGFP SNI $n = 6$ mice includes eGFP $n = 2$ mice, AKAPWT $n = 4$ mice; AKAPΔPP2B+SNI $n = 6$ mice; $*P < 0.05$,

$P < 0.001$ Student's *t* test. (**I**) Summary of effects of GalR1 KD and AKAPΔPP2B expression on nose pokes per day after model induction (data pooled from Figs. 1, 5, and 6) (*$P < 0.05$,$P < 0.001$ post hoc *t* test versus control; ++$P < 0.01$, +++$P < 0.001$ Tukey's post hoc *t* test versus respective pain model). (**J**) Schematic summarizing temporal order of synaptic and behavioral changes after pain induction.